IL NUOVO CIMENTO **40 C** (2017) 165
DOI 10.1393/ncc/i2017-17165-7

COLLOQUIA: LaThuile 2017

Right-handed neutrinos: DM and LFV *vs.* collider

M. CHEKKAL([1]), A. AHRICHE([2]), A. B. HAMMOU([1]) and S. NASRI([3])

([1]) *Department of Physics, University of Sciences and Technology of Oran - BP 1505, Oran, El M'Naouer, Algeria*
([2]) *Department of Physics, University of Jijel - PB 98 Ouled Aissa, DZ-18000 Jijel, Algeria*
([3]) *Department of Physics, United Arab Emirates University - Al-Ain, United Arab Emirates*

received 16 September 2017

Summary. — In a class of neutrino mass models with a lepton flavor violation (LFV) Yukawa interaction term that involves a heavy right-handed neutrino, a charged scalar and a charged lepton, we investigate at the ILC@500 GeV the possibility of observing news physics. These models can address neutrino mass and dark matter without being in conflict with different LFV constraints. By imposing DM relic density and LFV constraints, we recast the analysis done by L3 Collaboration at LEP-II of monophoton searches on our space parameter and look for new physics in such channels like monophoton and $SS(\gamma)$, where we give different cuts and show the predicted distributions. We show also that using polarized beams could improve the statistical significance.

1. – Introduction

Neutrino oscillations have been put in evidence by different experiences and observations caused by nonzero neutrino masses and neutrino mixing [1]. However, the Standard Model (SM) does not explain the intrinsic properties of neutrinos such as their origin, nature and the smallness of their masses. The seesaw mechanism [2] is the most popular method to explain the tiny mass of SM neutrinos but poses scale problems and prevents the direct detection of the right-handed (RH) neutrinos introduced by this mechanism because of its large mass compared to the electroweak scale.

The radiative neutrino mass models [3-7] is another way to generate a small mass to light neutrinos at loop level and to circumvent the scale problem. The violation of the leptonic number is permitted by the fact that the neutrinos are Majorana particles where the lightest RH neutrino is identified as being the dark matter and have large phenomenological implications. We can take as an example the model in [8] where authors show that the scale of new physics can be in the sub-TeV for the 3-loops neutrino mass generation model [6] which makes it testable at collider experiments [9]. In this work, we study the possibility of detecting the manifestations of the new physics resulting from this class of radiative neutrino mass models.

2. – LFV and DM constraints class of models with RH neutrinos

A class of radiative neutrino mass models are considered here, which are extending the SM with three right-handed neutrinos N_i $(i = 1, 2, 3)$ and a $SU(2)_L$-singlet charged scalar $S^{\pm}$. The models contain the following Yukawa term in in the Lagrangian [5-7, 10]

$$\mathcal{L}_{\mathcal{N}} \supset -\frac{1}{2} m_{N_i} \overline{N_i^c} P_R N_i + g_{i\alpha} S^+ \overline{N_i} \ell_{\alpha_R} + \text{h.c.}, \tag{1}$$

where ℓ_{α_R} is the right-handed charged lepton and $g_{i\alpha}$ are Yukawa couplings. The stability of the lightest RH neutrino, which is supposed to play the DM role, is assured by imposing the global Z_2 symmetry([1]). $\ell_\alpha \to \ell_\beta \gamma$ and $\ell_\alpha \to 3\ell_\beta$ are LFV processes produced by this type of interaction.

The contribution of the interactions (1) to the $\ell_\alpha \to \ell_\beta \gamma$ branching ratio is given by [12]

$$\mathcal{B}^{(N)}(\ell_\alpha \to \ell_\beta \gamma) = \frac{3(4\pi)^3 \alpha}{4 G_F^2} |A_D|^2 \times \mathcal{B}(\ell_\alpha \to \ell_\beta \nu_\alpha \bar{\nu}_\beta), \tag{2}$$

where α is the electromagnetic fine structure constant, G_F is the Fermi constant and A_D is the dipole contribution given by

$$A_D = \sum_{i=1}^{3} \frac{g_{i\beta}^* g_{i\alpha}}{2(4\pi)^2} \frac{1}{m_S^2} F\left(x_i\right), \tag{3}$$

where $x_i = m_{N_i}^2 / m_S^2$ and $F(x)$ is a loop function.

We scanned over all the free parameters of our model to determine the phenomenological implications for the dark matter and the searches of new physics at colliders. To get a feeling of the different contributions from the RH neutrino couplings, we define the ratio (fine-tuning parameter)

$$R = \frac{| \sum_{i=1}^{3} g_{i\mu}^* g_{ie} F\left(x_i\right) |^2}{\text{Max}[| g_{i\mu}^* g_{ie} F\left(x_i\right) |^2]}, \tag{4}$$

which represents the way the cancellation between different combinations $g_{i\beta}^* g_{i\alpha}$ occurs in order to suppress the LFV branching ratios even for large g-couplings. For instance, the parameter R could be significantly smaller than unity due to possible cancellation between different RH neutrinos contributions, and this may allow the g-couplings to be relatively large.

In fig. 1, for different values of fine-tuning parameter $R \approx\ 1,\ 10^{-2},\ 10^{-4}$, the branching ratios for the processes $\ell_\alpha \to \ell_\beta \gamma$ and $\ell_\alpha \to 3\ell_\beta$ *vs.* the charged scalar mass are presented. The experimental bounds of all branching fractions are the first constraint to be obeyed by the free parameters of the model, and some hundreds of configurations of free parameters are generated in this way.

([1]) The global Z_2 symmetry is accidental for higher representation (setplet) of RH neutrinos [11].

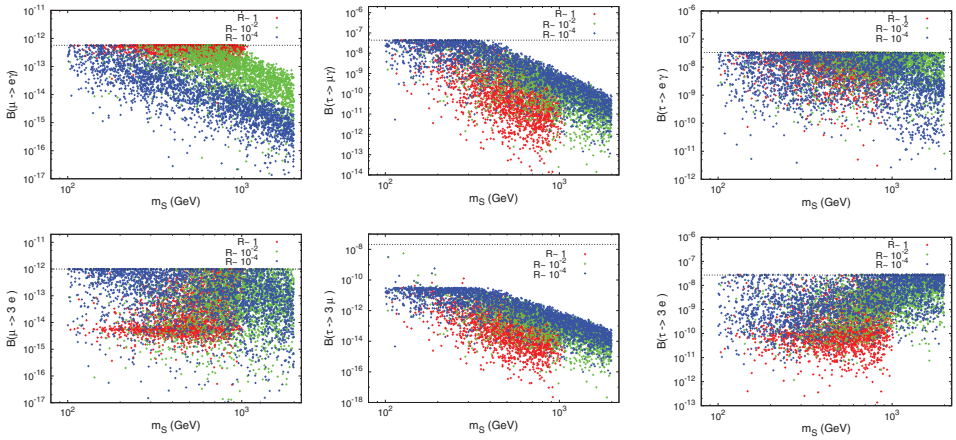

Fig. 1. – The branching ratios (top) $\mathcal{B}(\mu \to e\gamma)$, $\mathcal{B}(\tau \to \mu\gamma)$ and $\mathcal{B}(\tau \to e\gamma)$; and (bottom) $\mathcal{B}(\mu \to 3e)$, $\mathcal{B}(\tau \to 3\mu)$ and $\mathcal{B}(\tau \to 3e)$ *vs.* m_S. The horizontal dashed lines show the current experimental upper bounds for each radiative decay.

As mentioned earlier, the dark matter condidate could be the lightest RH neutrinos N_1 which is supposed stable. We can safely keep only the contribution of N_1 density and neglect that of N_2 and N_3 in the hierarchical RH neutrino mass spectrum case. The annihilation process $N_1 N_1 \to \ell_\alpha \ell_\beta$ via t-channel exchange of $S^\pm$ impoverished the density of N_1. When the temperature of the universe drops below the freeze-out temperature, and using the Boltzmann equation, we can approximate the relic density after the decoupling of N_1 from the thermal bath [13]

$$\Omega_{N_1} h^2 \simeq \frac{2x_f \times 1.1 \times 10^9\,\mathrm{GeV}^{-1}}{\sqrt{g^*} M_{pl} \langle \sigma_{N_1 N_1} v_r \rangle} \simeq \frac{17.56}{\sum_{\alpha,\beta} |g_{1\alpha} g^*_{1\beta}|^2} \left(\frac{m_{N_1}}{50\,\mathrm{GeV}}\right)^2 \frac{\left(1 + m_S^2/m_{N_1}^2\right)^4}{1 + m_S^4/m_{N_1}^4}, \tag{5}$$

In fig. 2, we present a contour plot m_{N_1} *vs.* m_S, where in palette we have the coupling combination $\sum_{\alpha\beta} |g_{1\alpha} g^*_{1\beta}|^2$, which appears in the expression of the relic density, with the conditions $m_{N_1} < m_S$ and $m_S > 100$ GeV being imposed. It is difficult to maintain all LFV ratios within the current experimental bounds for values of coupling combination larger than 10, and it requires an extreme fine-tunning. So, once the relic density are imposed and m_{N_1} and m_S are defined the $\sum_{\alpha\beta} |g_{1\alpha} g_{1\beta}|^2$ imposes another condition in addition to LFV constraint and the most viable range of the masses is extracted as $m_{N_1} < 200\,\mathrm{GeV}$ and $m_S < 300\,\mathrm{GeV}$.

3. – Constraints from LEP-II

An additional constraint on the free parameters is imposed by the lack of evidence for massive neutral particle realized by the L3 detector at LEP-II [14], which has conducted an analysis on single and multi photon events with missing for center-of-mass energies between 189 and 209 GeV. Indeed, benchmark points that respect the different DM and LFV constraints together must also give non-relevant significance under the same conditions as those of LEP.

In the next sections, we will carry out the electron-positron (electron-electron) collision on the ILC, so the decay length of the unstable particles N_2 and N_3 must then be

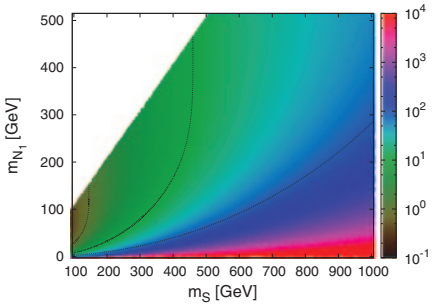

Fig. 2. – Dark matter mass *vs.* the charged scalar mass, The palette represents the quantity $\sum_{\alpha\beta}\left|g_{1\alpha}g^*_{1\beta}\right|^2$. The dashed curves (from left to right) represent the values $\sum_{\alpha\beta}\left|g_{1\alpha}g^*_{1\beta}\right|^2 = 1,\ 10,\ 100$, respectively.

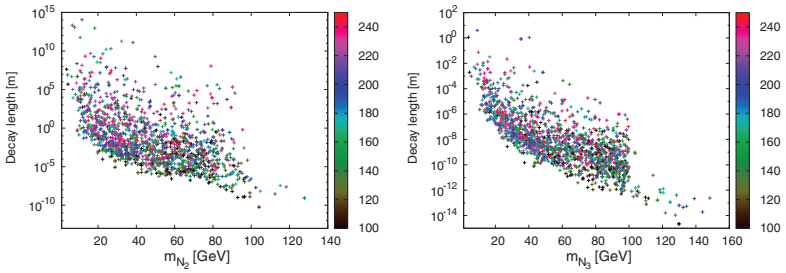

Fig. 3. – The decay length of the RH neutrinos N_2 (left) and N_3 (right) as a function of m_{N_2} and m_{N_3}, respectively. The palette represents the charged scalar mass m_S [GeV].

measured to determine whether they are disintegrating inside or outside the detectors. From fig. 3, it can be seen that N_3 does not contribute to the missing energy, being disintegrated mainly inside the detectors, whereas a substantial amount of N_2 events escape from the detector. In all our analysis the benchmarks points are verified in order to precisely identify the missing energy.

We consider the highest integrated luminosities $176\,\mathrm{pb}^{-1}$ and $130.2\,\mathrm{pb}^{-1}$ at the center-of-mass energies $\sqrt{s} = 188.6\,\mathrm{GeV}$ and $\sqrt{s} = 207\,\mathrm{GeV}$, respectively. The same kinematical cuts used by the L3 Collaboration for a high energy single photon are applied [14]: $|\cos\theta_\gamma| < 0.97$, $p_t^\gamma > 0.02\sqrt{s}$ and $E_\gamma > 1$ GeV. We compute the cross sections of the signal $e^-e^+ \to \gamma + E_{miss}$ and the background $e^-e^+ \to \nu_i\bar{\nu}_j\gamma$ using the LanHEP/CalcHEP packages [15, 16], for thousands of the aforementioned benchmark points.

The results are shown in fig. 4, where in palette one can read Δ, a quantity at which the cross-section is sensitive. An exclusion bound on a combination of these parameter is derived according to LEP analysis and the significance S must be smaller than three, thereby we extract the following constraint:

$$\Delta = \sum_{i,k} |g_{ie}g^*_{ke}|^2 \left[\frac{150\,\mathrm{GeV}}{m_S}\right]\left[\frac{50\,\mathrm{GeV}}{\sqrt{m_{N_i}m_{N_k}}}\right] < 1.95. \tag{6}$$

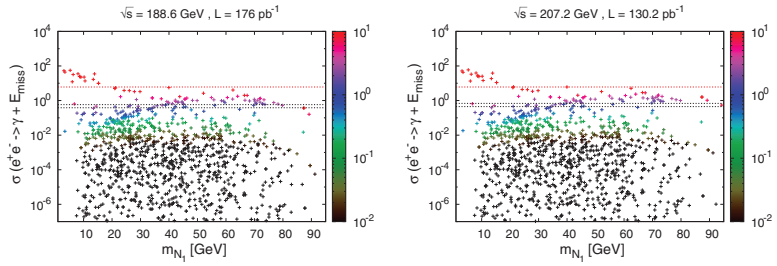

Fig. 4. – The cross section for the randomly chosen benchmark points for the process $e^-e^+ \to \gamma + E_{miss}$ at LEP as a function of m_{N_1} for the CM energies $\sqrt{s} = 188.6\,\text{GeV}$ (right) and $\sqrt{s} = 207.2\,\text{GeV}$ (left). The palette represents the combination Δ, and the black dashed lines correspond to $S = 2,\ 3$, respectively. The red dashed line corresponds to the background.

4. – Possible signatures at lepton colliders

In this work, we are interested in the possibility of probing new physics through charged scalar mediated processes that involve dark matter (missing energy) in the final state, at lepton colliders, especially the International Linear Collider (ILC) [17] which covers center-of-mass (CM) energies from 250 to 500 GeV. We study the most interesting

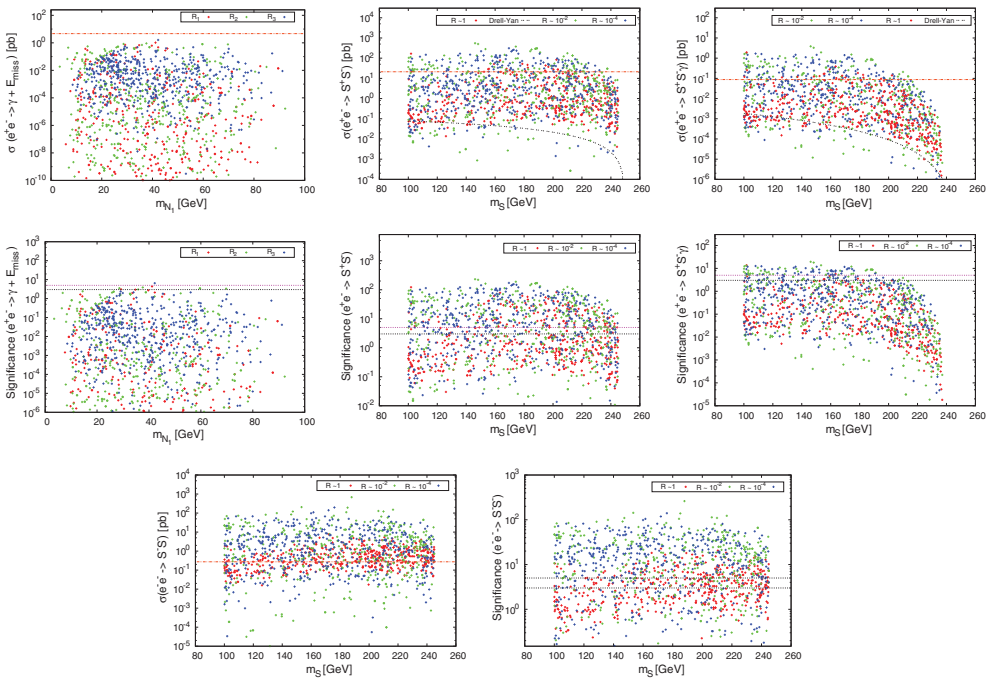

Fig. 5. – The cross section values (top) and the corresponding significance values (middle) for production via electron-positron collision and at bottom for production via electron-electron collision at luminosity $100\,\text{pb}^{-1}$ in function of m_S. The red lines represent the background value and the dashed one represents the Drell-Yann contribution in cross section, and the dashed lines represent $S = 3, 5$ in significance, respectively.

TABLE I. – *Three benchmark points selected from the parameters space of the model.*

Point	$B_1\,(R_1)$	$B_2\,(R_2)$	$B_3\,(R_3)$
g_{1e}	$(7.506 + i0.014) \times 10^{-1}$	$(1.8284 + i0.103)$	$(-0.103 + i0.201)$
g_{2e}	$(-0.26819 - i1.5758) \times 10^{-4}$	$(1.543 + i3.004) \times 10^{-4}$	$(0.654 - i2.616) \times 10^{-2}$
g_{3e}	$(-1.360 - i0.707)$	$(0.313 - i0.549)$	$(-0.869 - i0.878)$
m_S(GeV)	196.75	242.81	104.47
m_{N_1}(GeV)	25.788	43.764	38.306
m_{N_2}(GeV)	28.885	58.182	56.481
m_{N_3}(GeV)	36.274	67.511	72.440

signatures which occur via the interactions in (1), and give the following processes:

$$
\begin{aligned}
&e^- e^+ \to \gamma + E_{miss},\\
&e^- e^+ \to S^+ S^- \to \ell_\alpha^+ \ell_\beta^- + E_{miss},\\
&e^- e^- \to S^- S^- \to \ell_\alpha^- \ell_\beta^- + E_{miss},\\
&e^- e^+ \to \gamma + S^+ S^- \to \gamma + \ell_\alpha^+ \ell_\beta^- + E_{miss}.
\end{aligned}
\tag{7}
$$

Three processes for electron-positron collision are analyzed; photon(s) with a pair of DM in the final state where the background contributing to the signal give left-handed neutrinos with photon, and a pair production of charged scalars S^+S^- with or without a photon in the final state, where each charged scalar decays into a RH neutrino and a charged lepton. The corresponding background comes from the process $e^+e^- \to W^+W^-$ where W decays into a light neutrino and a charged lepton. Another potential signature comes from electon-electron collison and gives the same sign pair of charged scalars. A first qualitative analysis is carried out on the four processes in (7), on three sets of benchmark points according to different values of the ratio R for a center-of-mass energy of $\sqrt{s} = 500\,\text{GeV}$ and with a luminosity $L = 100\,\text{pb}^{-1}$. The cross section values and the corresponding significance are shown in fig. 5 *vs.* the charged scalar mass without applying any cut([2]). One remarks that the cross section values of the processes (7) in fig. 5 vary over seven orders of magnitudes as its sensitivity depends on our choice of the parameters space. The production cross section via electron-electron collision is large compared to the background, so even for low luminosity the significance is huge. Hence, the process with same sign charged scalars is a clean signal at the ILC. Detectability of production via electron-positron collision is developed in more detail in the next chapter.

([2]) Except for the cut $E_\gamma > 8\,\text{GeV}$ and $|\cos\theta_\gamma| < 0.998$ on channels with photon in the finale state.

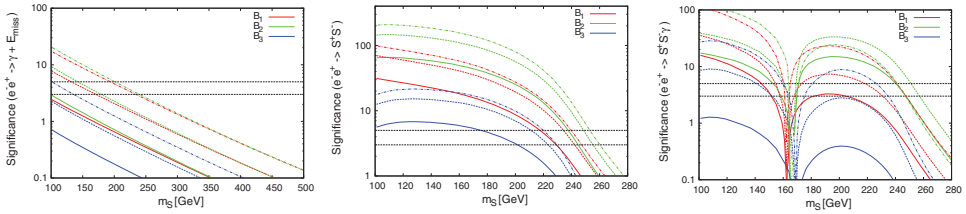

Fig. 6. – The signal significance for the processes $e^-e^+ \to \gamma + E_{miss}$ (left), $e^-e^+ \to S^-S^+$ (middle) and $e^-e^+ \to S^-S^+ + \gamma$ (right) as a function of m_S for the values of $g_{i\alpha}$ given table I at integrated luminosity of 1/10/10 (solid), 5/50/100 (dashed) and 10/100/500 (dash-dotted) fb^{-1}, respectively. The horizontal dashed lines correspond to a 3 and 5 sigma significance. For the values $m_S > 250\,\text{GeV}$, the charged scalar is off-shell.

5. – Benchmark analysis

Let us now consider three benchmarks points, one of each ratio $R_1 \approx 1,\ R_2 \approx 10^{-2}$ and $R_3 \approx 10^{-4}$, with nearby heavy neutrinos masses relatively. As can be seen on table I, our freedom of the model parameters space are substantially limited by the choice of the ratios R_i. The distributions for different kinematic variables are generated for signal and background using CalcHEP [16] for the processes $e^-e^+ \to \gamma + E_{miss}$, $e^-e^+ \to S^-S^+$, and $e^-e^+ \to S^-S^+ + \gamma$ at 500 GeV. We extract the optimal kinematical cuts for each process and this can be achieved as follows:

$$\text{final state } \gamma + E_{miss}\text{: } 8\,\text{GeV} < E_\gamma < 300\,\text{GeV},\ |\cos\ \theta_\gamma| < 0.998 \\ \text{and } E_{miss} > 300\,\text{GeV};$$

$$\text{final state } S^+S^-\text{: } M_{\ell^+,\ell^-} < 300\,\text{GeV},\ 150\,\text{GeV} < E_{miss} < 420\,\text{GeV}, \\ 30\,\text{GeV} < E^\ell < 180\,\text{GeV} \text{ and } p_t^\ell < 170\,\text{GeV};$$

$$\text{final state } S^+S^-\gamma\text{: } M_{\ell^+,\ell^-} < 300\,\text{GeV},\ 150\,\text{GeV} < E_{miss} < 400\,\text{GeV}, \\ 30\,\text{GeV} < E^\ell < 170\,\text{GeV},\ p_t^\ell < 170\,\text{GeV},\ |\cos(\theta_\gamma)| < 0.5, \\ 8\,\text{GeV} < E^\gamma < 120\,\text{GeV} \text{ and } p_t^\gamma < 110\,\text{GeV}.$$

By varying the charged scalar mass, the significance for these processes for the three considered benchmark points are shown in fig. 6 at integrated luminosity that brings us closer to 5 sigma significance for each channel. For the monophoton process, the signal

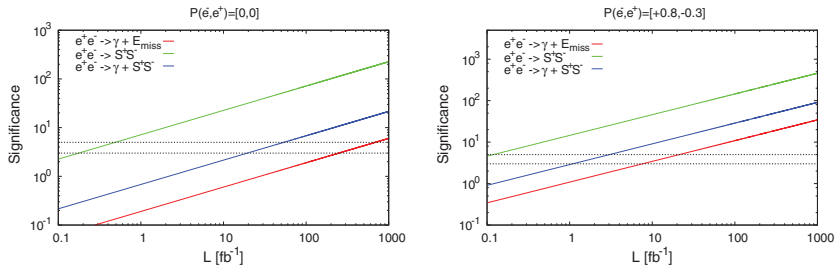

Fig. 7. – The signal significance as function of luminosity for the three different signatures studied, at left without polarization and at right with polarization of $P(e^-, e^+) = [+0.8, -0.3]$. The two horizontal dashed lines correspond to to a 3 and 5 sigma significance, respectively.

significance becomes detectable at the ILC for an integrated luminosity of a few hundred fb^{-1}. A luminosity of a few tens fb^{-1} is necessary to probe the production of a pair charged scalars with a photon while the S^-S^+ channel could be visible easily at very low luminosity, around 0.5 fb^{-1}. The charged scalar mass must be lighter than about 220 GeV in all these channels

There is an additional feature allowing the improvement of detection and which is available on the ILC, the possibility to have highly polarized electron/positron beams. A longitudinal polarization of 80% for the electron beam and 30% for the positron beam are planned by the ILC. We re-analyze the processes discussed earlier with all the possible polarizations combinations in order to improve the signal-background ratio and we found that for polarized beams as $P\,(e^-, e^+) = [+0.8, -0.3]$ while applying the same cuts used previously, the number of background events gets reduced by 86% and the signal increased by 130%. In fig. 7, we present the significance for $P(e^-, e^+) = [0, 0]$ and $P(e^-, e^+) = [+0.8, -0.3]$, for the benchmark point B_3 as a function of luminosity. One can note that the signal over background gets improved and the required integrated luminosity is dictated by a factor about ten for each processes studied.

6. – Conclusion

This paper investigates the behavior of some type of interaction present in a class of models that extends the standard model by majorana right-handed neutrinos and sclaire charged, to explain violations of leptonic flavor on one side, and to give a serious condidat to the dark matter of another. After imposing several constraints on the free parameters of models and carrying out an in-depth analysis on the detectability of the major processes resulting from the electron-positron collision in the conditions of the future lepton collider: ILC, we show that this type of interaction is likely to be probed, for different luminosity according to the final state, but which are all largely within the scope of the ILC capacity. It is also shown that the polarization of the electon/positron beams present in this collider can lead to a positive result very quickly.

* * *

MC wants to thank the organizers for the finanicial support. AA is supported by the Algerian Ministry of Higher Education and Scientific Research under the CNEPRU Project No. B00L02UN180120140040.

REFERENCES

[1] Super-Kamiokande Collaboration (Fukuda Y. *et al.*), *Phys. Rev. Lett.*, **81** (1998) 1562, arXiv:hep-ex/9807003; OPERA Collaboration (Agafonova N. *et al.*), *JHEP*, **11** (2013) 036; **04** (2014) 014(E), arXiv:1308.2553 [hep-ex]; Batkiewicz M. for the T2K Collaboration, arXiv:1705.04277 [hep-ex].

[2] Gell-Mann M., Ramond P. and Slansky R., in *Supergravity*, edited by van Nieuwenhuizen P. and Freedman D. Z. (North-Holland) 1979, p. 315; Yanagida T., in *Proceedings of the Workshop on the Unified Theory and the Baryon Number in the Universe*, edited by Sawada O. and Sugamoto A., KEK Report No. 79-18 (Tsukuba, Japan) 1979, p. 95; Mohapatra R. N. and Senjanovic G., *Phys. Rev. Lett.*, **44** (1980) 912.

[3] Zee A., *Phys. Lett. B*, **161** (1985) 141.

[4] Zee A., *Nucl. Phys. B*, **264** (1986) 99; Babu K. S., *Phys. Lett. B*, **203** (1988) 132.

[5] Ma E., *Phys. Rev. D*, **73** (2006) 077301, arXiv:hep-ph/0601225.

[6] Krauss L. M., Nasri S. and Trodden M., *Phys. Rev. D*, **67** (2003) 085002, arXiv:hep-ph/0210389.
[7] Aoki M., Kanemura S. and Seto O., *Phys. Rev. Lett.*, **102** (2009) 051805, arXiv:0807.0361 [hep-ph]; *Phys. Rev. D*, **80** (2009) 033007, arXiv:0904.3829 [hep-ph].
[8] Ahriche A., Chen C. S., McDonald K. L. and Nasri S., *Phys. Rev. D*, **90** (2014) 015024, arXiv:1404.2696 [hep-ph]; Ahriche A., McDonald K. L. and Nasri S., *JHEP*, **10** (2014) 167, arXiv:1404.5917 [hep-ph]; **02** (2016) 038, arXiv:1508.02607 [hep-ph].
[9] Ahriche A., Nasri S. and Soualah R., *Phys. Rev. D*, **89** (2014) 095010, arXiv:1403.5694 [hep-ph]; Guella C., Cherigui D., Ahriche A., Nasri S. and Soualah R., *Phys. Rev. D*, **93** (2016) 095022, arXiv:1601.04342 [hep-ph]; Cherigui D., Guella C., Ahriche A. and Nasri S., *Phys. Lett. B*, **762** (2016) 225, arXiv:1605.03640 [hep-ph].
[10] Okada H. and Yagyu K., *Phys. Rev. D*, **93** (2016) 013004, arXiv:1508.01046 [hep-ph]; Jin L. G., Tang R. and Zhang F., *Phys. Lett. B*, **741** (2015) 163, arXiv:1501.02020 [hep-ph]; Cheung K., Nomura T. and Okada H., arXiv:1610.04986 [hep-ph]; Baek S., Okada H. and Toma T., *J. Cosmol. Astropart. Phys.*, **06** (2014) 027, arXiv:1312.3761 [hep-ph]; Kashiwase S., Okada H., Orikasa Y. and Toma T., *Int. J. Mod. Phys. A*, **31** (2016) 1650121, arXiv:1505.04665 [hep-ph]; Kanemura S., Nishiwaki K., Okada H., Orikasa Y., Park S. C. and Watanabe R., *Prog. Theor. Exp. Phys.*, **2016** (2016) 123B04, arXiv:1512.09048 [hep-ph]; Kanemura S., Seto O. and Shimomura T., *Phys. Rev. D*, **84** (2011) 016004; Ahriche A., McDonald K. L. and Nasri S., *JHEP*, **02** (2016) 038, arXiv:1508.02607 [hep-ph]; **06** (2016) 182, arXiv:1604.05569 [hep-ph].
[11] Ahriche A., McDonald K. L., Nasri S. and Toma T., *Phys. Lett. B*, **746** (2015) 430, arXiv:1504.05755 [hep-ph].
[12] Toma T. and Vicente A., *JHEP*, **01** (2014) 160, arXiv:1312.2840 [hep-ph]; Hisano J., Moroi T., Tobe K. and Yamaguchi M., *Phys. Rev. D*, **53** (1996) 2442, arXiv:hep-ph/9510309.
[13] Ahriche A. and Nasri S., *J. Cosmol. Astropart. Phys.*, **07** (2013) 035, arXiv:1304.2055 [hep-ph].
[14] L3 Collaboration (Achard P. *et al.*), *Phys. Lett. B*, **587** (2004) 16, arXiv:hep-ex/0402002.
[15] Semenov A., *Comput. Phys. Commun.*, **201** (2016) 167, arXiv:1412.5016 [physics. comp-ph].
[16] Belyaev A., Christensen N. D. and Pukhov A., *Comput. Phys. Commun.*, **184** (2013) 1729, arXiv:1207.6082 [hep-ph].
[17] Baer H. *et al.*, arXiv:1306.6352 [hep-ph].